NANOSTRUCTURED Y_2O_3 PARTICLES DOPED WITH EUROPIUM SYNTHESIZED BY AEROSOL ROUTE

Luz Stella Gomez[1], Katarina Marinkovic[2], Jose Manuel Torralba[1], Maria Eugenia Rabanal[1] & Olivera Milosevic[2]

[1]Universidad Carlos III de Madrid, Avda. de la Universidad 30, Spain
[2]Institute of Technical Sciences of Serbian Academy of Sciences and Arts, K.Mihailova 35/IV, 11000 Belgrade, Serbia

Corresponding author: Olivera Milosevic, olivera.milosevic@itn.sanu.ac.rs

Abstract: Y_2O_3 doped with europium is a well known red phosphor material employed in modern high-resolution display devices such as plasma display panels (PDP) and field emission displays (FED). The incorporation of gadolinium in the yttria matrix may significantly contribute to the luminescent properties and x-ray absorption coefficient thus increasing the field of application in optoelectronic devices such as ceramic scintillators for computed tomography. In this work, the nanostructured particles of Y_2O_3 doped with Eu^{3+} were processed through the spray pyrolysis method. Synthesis was carried out with an ultrasonic aerosol device operating at 1.3 MHz in air atmosphere connected with a triple-zone tubular flow reactor (473-973-1173K). Particles were submitted to post-thermal treatments at temperatures among 1273 and 1573K for 12 hours in order to increase the crystallinity and uniform distribution of doped centers. Morphology, structure, crystallinity and chemical characteristics were studied by XRD, SEM-EDS, TEM-HRTEM and SAED. The particles obtained are spherical, having narrow size distributions, high compositional homogeneity and are in un-agglomerated state. The effects of synthesis parameters were followed and discussed in terms of particle structure and morphology.

Key words: Nanostructured ceramic materials, spray pyrolysis.

1. INTRODUCTION

Luminescent materials represent inorganic crystalline structures capable of emitting definite quantities of radiation within visible and/or ultraviolet spectrum as a result of excitation by an external energy source such as electron or a photon beam (Rack & Holloway, 1998; Ropp, 1991). Such properties of these materials are an outcome from the atomic state interactions that occur between luminescent centers and the host lattice material after the excitation. Rare earth ions ($Eu^{2+,\ 3+}$, Ce^{3+}, $Tm^{3+,}$ Tb^{3+}, Nd^{3+}) and transition metal ions (Cr^{3+}, Mn^{2+}) are commonly used as luminescent centers (Kang et al., 2000; Maghrabi et al., 2001). Luminescent materials are normally utilized in cathode ray tubes for television screens and due to excellent characteristics of these materials their use has increased in the past years due to their application in modern emissive display industry such as flat screens, plasma and electroluminescence screens, etc. The most important properties that luminescent materials should possess are their brightness, spectral energy distribution and decay time (Zych et al., 1997).

The interest of the Y_2O_3 has been broadly known due to its particularly relevant physical and functional properties, including the crystallographic stability, a wide band energy gap (5.5e.v.) and the ability to be a host material for rare earth atoms.

Yttrium oxide is a good phosphor material with different luminescent spectra depending on the luminescent center by which it is activated (for example Eu, Tb, Dy, Tm or Nd); doped with Eu^{3+} is a well known red phosphor in flat panel displays (Bhargave et al., 1994; Wan et al., 2005; Tissue & Yuan, 2003).

In particular, it has been shown that if in nanostructure form it possesses improved quantum efficiency (Allieri et al., 2000) while the mixed oxide with rare earth ions (Re), the $Re_xY_{2-\ x}O_3$ type, represents a new group of superconducting materials (Mitric et al., 1993).

Yttria represents one of the best host materials for rare earth ions due to the fact that its ionic radii and crystal structure are very similar to the ionic radii and crystal structure of the rare earth ions (Kang et al., 1999). There are several crystal structures of Y_2O_3: cubic, type Mn_2O_3, which represents a stable equilibrium structure under stationary conditions and monoclinic structure with space group *C2/m* that can be formed under extreme synthesis conditions such as high temperature (Dosev et al., 2006; Wang et al., 2006).

Having all this in mind the development of modern luminescent materials is connected in a great deal to the development of adequate and applicable synthesis method and in this context high structural and morphological requirements are appointed and they should be obtained from a specific synthesis method (Rao, 1996; McKittrick et al., 1999).

The requirements that need to be achieved are uniform luminescent center distribution throughout the host lattice, high phase crystallinity, a small particle size with a narrow size distribution, high

particle surface area, spherical morphology and absence of agglomerates (Kang et al., 1999; Milosevic et al., 2005).
Several synthesis techniques have been used to design nanostructured materials including procedures such as sol-gel (Zhang et al., 2002; Murillo, 2002) chemical synthesis (Igarashi et al., 2000), flame spray pyrolysis (Kang et al., 2001), or hydrothermal and solvothermal precipitation (Guo et al., 2004).
In comparison to other synthesis methods, powder synthesis through aerosol route (spray pyrolysis) enables formation of very fine submicronic, nanostructured particles that can be either single or multi component oxide materials formed from a range of precursor solutions (Messing et al., 1993; Gurav et al., 1993; Kang et al., 2001). This process implies formation of discreet aerosol droplets and the control over their thermal decomposition in high temperature tubular flow reactor. The aerosol is usually formed by an ultrasound of high frequency (100 KHz-10MHz) and the average droplet size depends on the applied frequency and on the solution parameters (viscosity, surface tension, concentration, density, etc.).
Based on our research in the field of the luminescent materials synthesis by spray pyrolysis conducted so far (Wang et al., 2006; Milosevic et al., 2005), one of the intends of this work was to apply the synthesis concept with the aim to reach the wanted crystal structure: cubic yttrium oxide for Y_2O_3:Eu^{3+} system and spherical morphology, since the latter may improve both the packing density and luminescence behavior.
The effect of dopant and synthesis parameters were monitored and discussed in terms of particle structure and morphology. A rigorous control of crystalline phases was carried out checking during all the synthesis process and post- treatments, focused to the stability of the cubic *Ia3* phase.

2. EXPERIMENTAL

Y_2O_3 doped with Eu^{3+} having 1.9:0.1 atomic (Y/Eu) ratio was synthesized through the spray pyrolysis method from 0.1M precursor solution of $Y(NO_3)\cdot 6H_2O$ and $Eu(NO_3)\cdot 5H_2O$. An ultrasonic aerosol generator (RBI, France) with a frequency of 1.7 MHz was used to atomize previously prepared nitrate precursor solution. The formed aerosol droplets were carried out using air as a carrier gas (flow rate of 1.0 l/min) and decomposed in a triple zone tubular flow reactor pre-setting at 473-973-1173K.
As-prepared powder samples, collected at the exhaust, were subjected to the post thermal treatments carried out at temperatures among 1273-1573K for 12 hours in order to increase the crystallinity and the homogeneity of doped centers.
X-ray diffraction (XRD), scanning electron microscopy (SEM), transmission electron microscopy (TEM), high resolution transmission electron microscopy (HRTEM) and selected area electron diffraction (SAED) were used for the morphological, chemical and structural characterization. Crystallographic phases were determined by combining the XRD results and the electron diffraction-HRTEM techniques, using the Morniroli procedure (Dosev et al., 2006; Morniroli&Steeds, 1992). HRTEM images were treated using the digital micrograph^{TM} program. A multi-slice method of images simulation was used to perform a model of high resolution images.
The simulation of high resolution electron microscope images is most often used to understand the contrast of experimental micrographs and to adjust a model structure to an experimental one (Wang et al., 2006). The comparison with the simulated images was carried out taking into account the imaging conditions under which the experimental image had been recorded, such as the local thickness (Δt), the defocus setting (Δf) of the objective lens, the beam tilt and specific parameters of the microscope (voltage, resolution, spherical aberration), and then determined by matching the simulated images to the experimental images along each zone axis orientation (Stadelman, 1995).
XRD patterns were recorded with CuK_α radiation in an X`Pert Philips automatic diffractometer. The 2Θ range analyzed was 10º to 80º with a step scan of 0.02 and a counting time of 10 s for each step. The working conditions were 40 kV and 40 mA. A Philips XL 30 scanning electron microscope equipped with secondary (SE), backscattered (BSE) and an energy dispersive X-ray (EDAX) detector was employed to study the microstructure and composition of the material. TEM samples were prepared by ultrasonic dispersion of a small powder portion in acetone and then disposed on a carbon coated copper grid with 3mm of diameter. A TEM JEOL JEM 4000 EX operated at 400 kV with a resolution of 1.8 Å was employed.

3. RESULTS

XRD data allowed identifying the crystalline phases and refining the cell parameters. Fig. 1a,b represents the XRD results obtained for the $Y_{1.9}Eu_{0.1}O_3$ samples. Fig 1a represents the evolution of the XRD patterns before and after annealing. The maximums are clearly defined and indexed according to the *Ia3* phase. (JCPDS= 43-1036, SG= 206).
Fig. 1b represents the Rietveld refinement for the sample after a thermal treatment at 1273K / 12 h showing the observed and calculated patterns and the peak difference for *Ia3* space group (reference values for Rietveld factors fit: 12<Rp<20, 13<Rwp<25, 3 <Rb<11, $\chi 2 \rightarrow 1$) (Rodríguez, 1990).

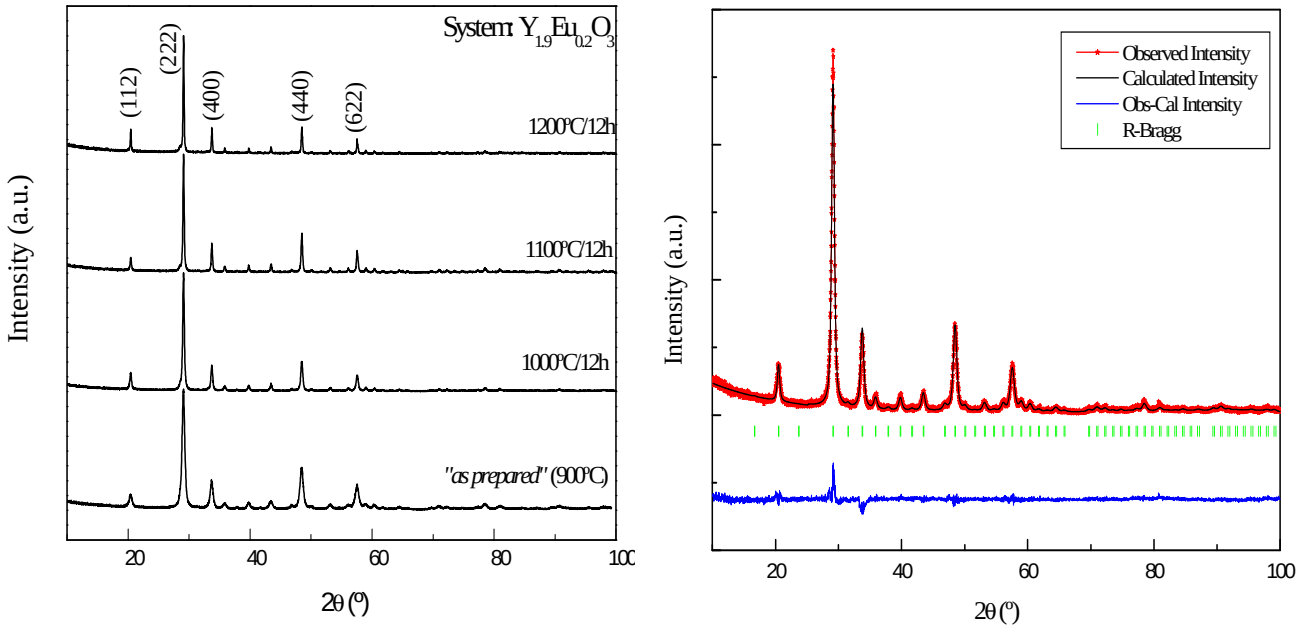

(a) (b)

Fig 1 Experimental X-ray diffraction patterns for as-prepared and thermally treated powder samples (a). The Rietveld refinement for the sample thermally treated at 1273K/12 h.

Table 1 summarizes the Rietveld based Fullprof refinement results for both the as-prepared and thermally treated powder samples. Adjustment goodness indices (Young & Wiles, 1982) reveal an adequate agreement between experimental and theoretical models for *Ia3* phase during annealing.

Table 1. The $Y_2O_3:Eu^{3+}$ structural parameters obtained by Rietveld refinement.

Temperature (K)/Time (h)	Cell parameter (Å)	Rb	Rf	Rp	Rwp	χ^2	Strains (10^{-3})%
"as prepared"		2.67	2.74.	6.77	9.35	1.24	18.7(±1.4)
1273/12	10.605(1)	5.02	9.43	8.52	12.3	1.55	9.81(±1.6)
1373/12	10.606(7)	6.73	7.58	9.53	13.7	1.69	5.99(±1.3)
1473/12	10.607(5)	10.7	19.9	12.2	16.7	1.98	4.99(±1.3)

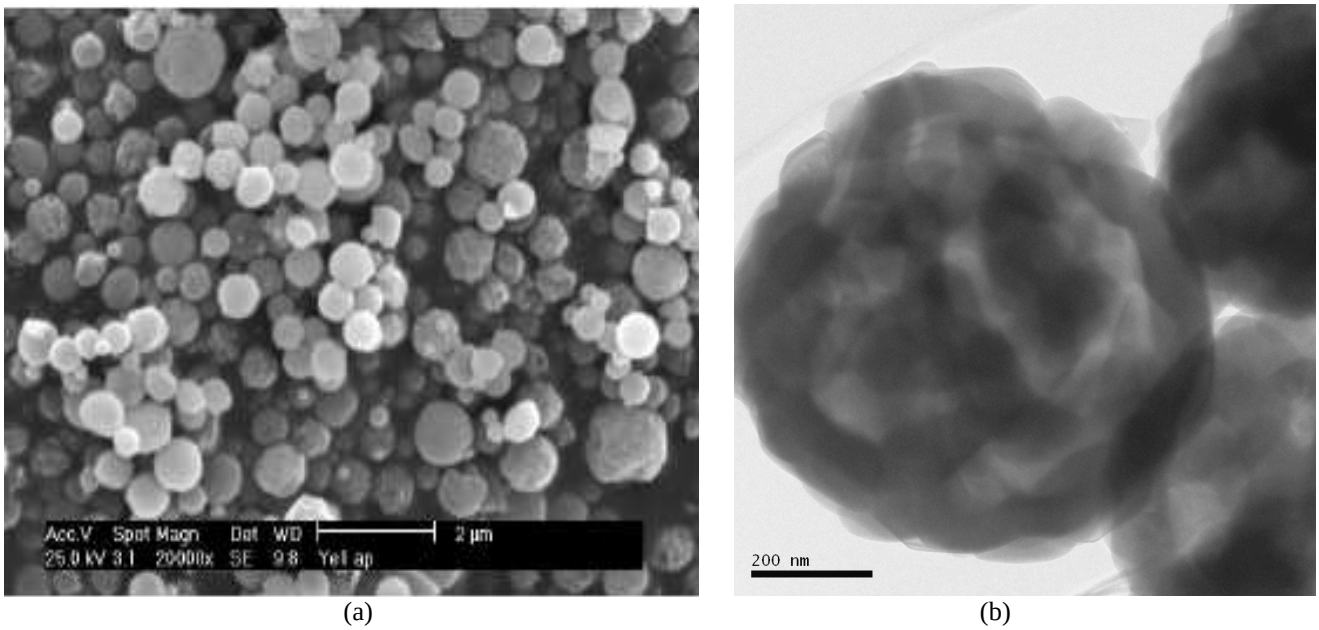

(a) (b)

Fig. 2. Scanning electron micrograph of the as-prepared powder sample (a); Low magnification TEM image in bright field mode of the same sample, thermally treated.

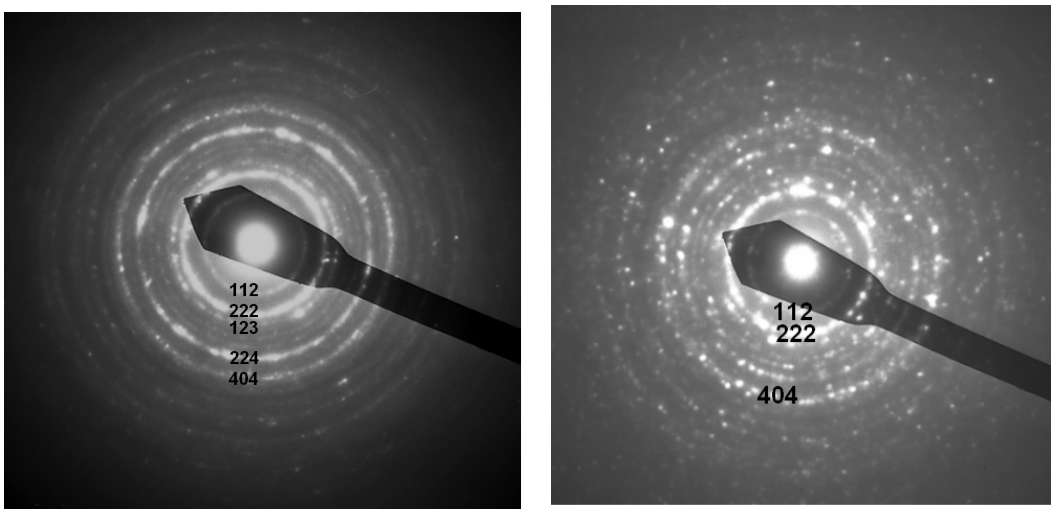

(a) (b)

Fig. 3. SAED ring pattern of the as-prepared (a), and thermally treated powder sample (1373K/12 h) (b) indexed according to *Ia3* phase.

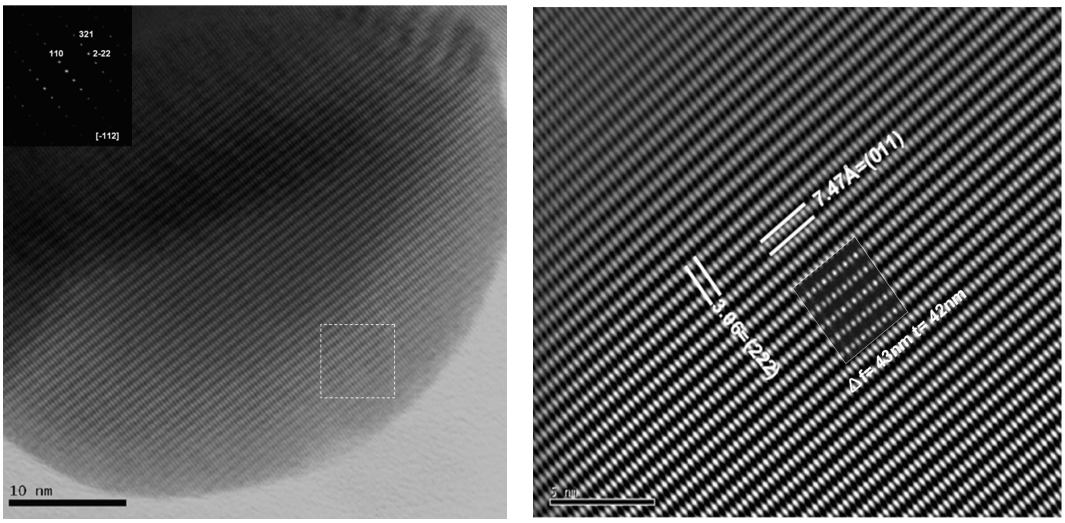

(a) (b)

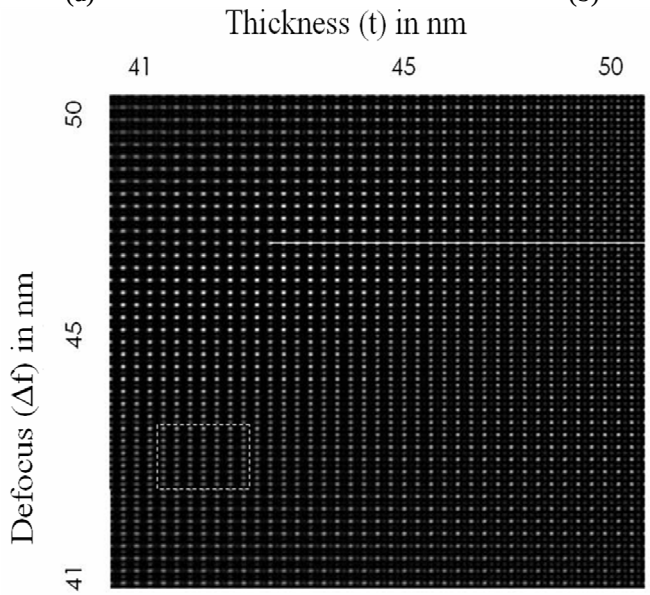

(c)

Fig. 4 HRTEM images of a nanoparticle thermally treated at 1473K/12 h, the *fft* image oriented at [-112] zone axis (inset, the upper left corner) (a); *fft* HRTEM image and the simulated image overlapped with defocus Δf=43 nm and thickness t=42 nm (b); Simulated images at different conditions of thickness (t) in nm (horizontal direction) and defocus (Δf) in nm (vertical direction) along the [-112] zone axis (TEM microscope operated at 400kV with a resolution of 1.8 Å) (c).

It is evident the cell parameter increase and strains decrease with the thermal treatment temperature.

In Fig. 2a, a secondary electron SEM image of as-prepared powder samples reveals the spherical, un-agglomerated, submicronic, so called "secondary" particles. Fig. 2b represents a low magnification bright field image identifying the secondary particle substructure composed of primary nanoparticles aroused trough the collision/coalescence mechanisms. Selected area electron diffraction (SAED) patterns of as-prepared and thermally treated (1273K) samples are presented at Fig. 3a, b. The ring patterns indicate the polycrystalline structure, while the textured character of the SAED pattern indicates high defect content. The *Ia3* phase is identified in both diffractograms and the main crystallographic planes are indexed. The differences in the ring breadth are related to the changes in the particle sizes. The Y_2O_3 *hkl* distances are in agreement with the cell parameters calculated by Fullprof programme (Rodríguez, 1990).

Fig 4a represents a HRTEM image in bright field mode of a particle treated at 1373K/12h. The fast fourier Transform (*fft*) of the image oriented along the [-112] zone axis is included as inset at the upper left corner (Fig. 4a). The *fft image* is shown as an enlargement in the Fig. 4b indicated a well ordered lattice.

The few defects present are associated to the intersection with other particle (the upper right corner, magnified in Fig.5a). The (011) and (222) atomic planes according to the *Ia3* phase are resolved. No intermediary phase is observed along the particles.

In order to confirm the *Ia3* phase in the HRTEM images, the experimental contrast was checked. Simulated images were calculated for different thickness (t) and defocus (Δf) values of the *Ia3* phase as is shown in Fig 4c.

The High resolution images map along the [-112] direction is represented. Thickness increases horizontally, defocus vertically. The best fit is found at t=42 nm and f=43 nm and the calculated image (overlapped) agrees well with the experimental one as is shown in Fig. 4b.

Fig 5a shows an enlargement of the area at the interfaces between two particles revealing the accommodation between two periodic lattices, with an array of dislocations along the interface locally forming moiré fringes. The filtered fourier HRTEM image revealing the accommodation between two primary particles is presented at Fig.5b. A small interruption in the periodicity along the interface is observed. The magnified region corresponding to the sintering neck between the primary particles is presented in inset.

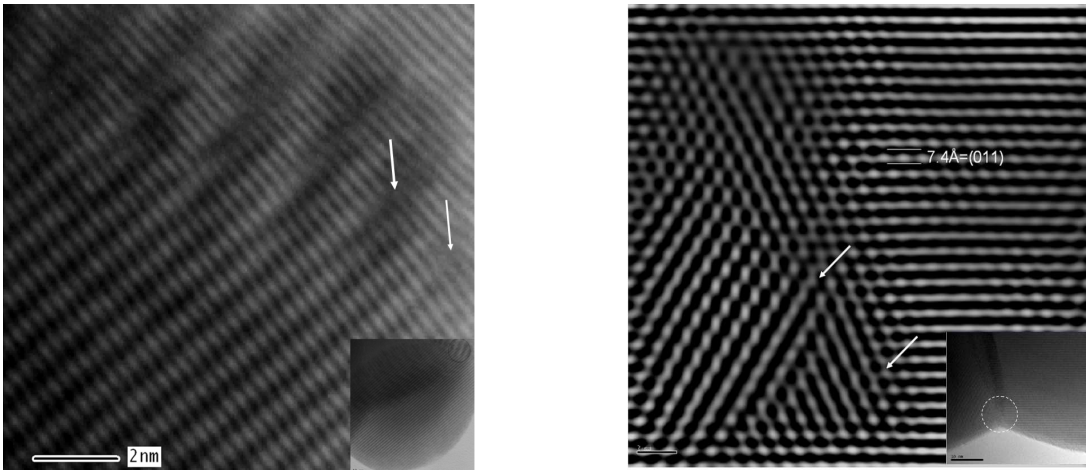

(a) (b)

Fig. 5. HRTEM *ifft* images at the interface between two primary particles showing a moiré fringe in the dislocation area. (a) and defects in the boundary area (b)

4. CONCLUSIONS

Nanostructured, spherical, un-agglomerated and homogeneous particles of Y_2O_3 doped with Eu^{3+} have been synthesized through spray pyrolysis route from common nitrate solution. The *Ia3* phase has been identified by XRD and TEM-HRTEM-SAED. No intermediate phase is observed along the particles. Strain fields don't affect the stability of this phase and only represents the attachment mechanisms between particles. These morphological and structural characteristics make this material to be promising for luminescent applications, particularly as red phosphor in flat panel displays.

Acknowledgments

The authors gratefully appreciate the financial support of the Ministry for Science and Technology, Serbia (Project #142010) and the assistance in TEM characterization of the Electron Microscopy Center, Universidad Complutense de Madrid, Spain.

5. REFERENCES

1. Allieri, B., Depero, L.E., Marino, A., Sangalleti, L.,.Caporaso, L, Speghini, A., Bettinelli, M. (2000),

Growth and microstructural analysis of nanosized Y_2O_3 doped with rare-earths, Mater. Chem .Phys., 66, 164
2. Bhargave R.N. Gallagher D. Welker T. (1994), *Doped nanocrystals of semiconductors-a new class of luminescent materials J. Lumin*., 61. 275
3. Dosev, D., Guo, B., Kennedy, I. M. (2006), *Photoluminscence of as an indication of crystal structure and particle size in Eu^{3+}: Y_2O_3 nanoparticles synthesized by flame spray pyrolysis, Aerosol Sci*., 37, 42
4. García Murillo A., (2002), *Elaboration, propriétés structurales, optiques et spectroscopiques de films sol-gel scintillants de Gd_2O_3 et Lu_2O_3 dopés Eu^{+3}* Tesis doctoral L'université Claude Bernard Lyon I. 173p.
5. Guo C.W. Cao Y. Xie S.H. Dai W.L. Fan K.N. (2004), *Structure and optical properties of sol-gel derived Gd_2O_3 waveguide films, A*pplied Surface Science, 230. 215-221
6. Gurav, A., Kodas, T., Pluym, T. and Xiong, Y. (1993), *Aerosol processing of materials*, Aerosol Sci. Technol., 19, 411
7. Igarashi T. Ihara M. Kusunoki T., Ohno K., (2000), *Relationship between optical properties and crystallinity of nanometer Y_2O_3:Eu phosphor*, Appl. Phys. Lett., 76. 1549.
8. Kang, Y. C., Park, S. B., Lenggoro, I. W. and Okuyama, K. (1999), *Gd_2O_3:Eu phospor particles with sphericity, submicron size and nonaggregation characterisitics*. J. Phys. Chem. Solids, 60, 379
9. Kang, Y. C., Park, S. B., Lenggoro, I. W. and. Okuyama, K (1999), *Morphology control of multicomponent oxide phosphor particles containing high ductility component by high temperature spray pyrolysis* J. Electrochem. Soc., 146, 2744
10. Kang, Y. C., Lenggoro, I. W., Park, S. B. and Okuyama, K. (2000), *YAG-Ce phosphor particles prepared by ultrasonic spray pyrolysis*, Mater. Res. Bull., 35, 789
11. Kang Y.C., Seo D.J. Park S.B. Park H.D. (2001), *Morphological and optical characteristics of Y_2O_3:Eu phosphor particles prepared by flame spray pyrolysis*, Jpn. J. Appl. Phys., 40. (1). 6 A, 4083-4086.
12. Kang, Y. C., Roh, H. S. and Park, S. B. (2001), *Sodium Carbonate Flux Effects on the Luminescence Characteristics of (Y0.5Gd0.5)2O3:Eu Phosphor Particles Prepared by Spray Pyrolysis* J. Am. Ceram. Soc., 84, 447
13. Maghrabi, M., Townsend, P. D., Vazquez, G. (2001) *Low temperature luminescence from the near surface region of Nd:YAG,*J. Phys.:Condens. Matter, 13, 2497.
14. McKittrick, J., Shea, L. E., Bacalski, C. F. and Bosze, E. J. (1999), *The influence of processing parameters on luminescent oxides produced by combustion synthesis*, Displays, 19, 169
15. Messing, G. L., Zhang, S.-C. and Jayanthi, G. V. (1993), *Ceramic powder synthesis by spray pyrolysis*, J. Am. Ceram. Soc., 76, 2707
16. Milosevic, O., Mancic, L., Rabanal, M.E., Yang, B. and Townsend, P.D. (2005), S*tructural and luminescence properties of Gd_2O_3:Eu^{3+} and $Y_3Al_5O_{12}$:Ce^{3+} phosphor particles synthesized via aerosol*, J. Electrochem. Soc., 152 (9), G707-G713
17. Mitric, M., Onnerud, P., Rodic, D., Tellgren, R., Szytula, A., Napijalo, M.Lj. (1993), *The preferential site occupation and magnetic properties of $Gd_xY_{2-x}O_3$*, J.Phys.Chem.Solids, 54, 967
18. Morniroli, J.P., Steeds, J. W., (1992), *Microdiffraction as a tool for crystal structure identification and determination*, Ultramicroscopy, 45, 219-239.
19. Rack, P. D., Holloway, P. H. (1998), *The structure, device physics, and material properties of thin film electroluminescent displays*, Mater. Sci. Eng., 4, 171.
20. Rao, R. P. (1996), P*reparation and characterization of fine grain yttrium based phosphors by sol-gel process* J. Electrochem. Soc., 143, 189
21. Rodríguez Carvajal, (1990), *Rietveld Pattern Matching Analysis of powder pattern*. ILLL Grenoble
22. Ropp, R. C. (1991), *Luminescence and the Solid State*, Elsevier Science Publishers B. V., New York
23. Tissue, B.M., Yuan, H.B.(2003), *Structure, particle size and annealing of gas-phase condensed Eu^{3+}: Y_2O_3 nanophosphors*, J.Solid State Chem., 171, 12
24. Stadelman Pierre, (1995), *Image calculation techniques package software*. Centre Interdépartemental de Microscopie Electronique, EPFL, Lausanne. CERN Webmaker.
25. Wan J. Wang Z., Chen X., Mu L., Qian Y. (2005), *Shape tailored photoluminescent intensity of red phosphor Y_2O_3:Eu^{3+}*. Journal of Crystal Growth., 284. 538-543.
26. Wang, Y., Milosevic, O., Gomez, L., Rabanal, M.E., Torralba, J.M., Yang, B., Townsend, P. D. (2006), *Thermoluminiscence responses from europium doped gadolinium oxide*, J. Phys.: Condens. Matter, 18, 9257
27. Young R.A., Wiles D.B. (1982), *A new computer program for Rietveldt analysis of X Ray powder diffraction patterns*, J. Appl. Cryst. 15, p.430
28. Zhang J., Tang Z., Zhang Z., Fu, W., Wang J. Lin Y. (2002), *Synthesis of nanometer Y_2O_3:Eu phosphor and luminescence property*. Material Science Engineering A., 334 246-249.
29. Zych, E., Brecher, C., Wojtowicz, A. J. and Lingertat, H. (1997), *Luminescence properties of Ce-activated YAG optical ceramic scintillator materials*, J. Lumin., 75, 193

Received: 16 November 2009 / Accepted: 20 December 2009 /
Abstract published online: 15 January 2010